




## Synthesis, characterization and comparative DNA interaction studies of new copper(II) and nickel(II) complexes containing mesalamine drug using molecular modeling and multispectroscopic methods

Nahid Shahabadi, Soraya Moradi Fili & Mohsen Shahlaei

To cite this article: Nahid Shahabadi, Soraya Moradi Fili & Mohsen Shahlaei (2015) Synthesis, characterization and comparative DNA interaction studies of new copper(II) and nickel(II) complexes containing mesalamine drug using molecular modeling and multispectroscopic methods, Journal of Coordination Chemistry, 68:20, 3667-3684, DOI: [10.1080/00958972.2015.1078897](https://doi.org/10.1080/00958972.2015.1078897)



To link to this article: <http://dx.doi.org/10.1080/00958972.2015.1078897>

 View supplementary material 

 Accepted author version posted online: 13 Aug 2015.  
Published online: 21 Aug 2015.

 Submit your article to this journal 

 Article views: 60

 View related articles 

 View Crossmark data 

## Synthesis, characterization and comparative DNA interaction studies of new copper(II) and nickel(II) complexes containing mesalamine drug using molecular modeling and multispectroscopic methods

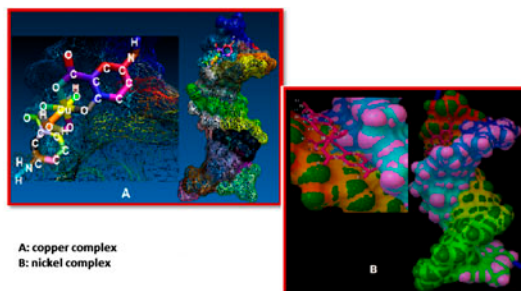
NAHID SHAHABADI\*<sup>†‡</sup>, SORAYA MORADI FILI<sup>†</sup> and MOHSEN SHAHLAEI<sup>§</sup>

<sup>†</sup>Faculty of Chemistry, Department of Inorganic Chemistry, Razi University, Kermanshah, Iran

<sup>‡</sup>Medical Biology Research Center (MBRC), Kermanshah University of Medical Sciences, Kermanshah, Iran

<sup>§</sup>Faculty of Pharmacy, Department of Medicinal Chemistry, Medical Sciences University, Kermanshah, Iran

(Received 11 December 2014; accepted 25 June 2015)



Complexes of copper(II) and nickel(II) containing the drug mesalamine (5-ASA) have been synthesized and characterized by FT-IR, mass and UV-vis spectra, elemental analysis, and theoretical methods. The binding interactions between mesalamine and its Cu(II) and Ni(II) complexes with calf thymus DNA (ct-DNA) were investigated using absorption, fluorescence emission and circular dichroism (CD) spectroscopies, and viscosity measurements. Absorption spectra of 5-ASA, Cu(II) and Ni(II) complexes showed hypochromism. The calculated binding constants ( $K_b$ ) obtained from UV-vis absorption studies were  $1.27 \times 10^3$ ,  $1.6 \times 10^3$ , and  $1.2 \times 10^4 \text{ M}^{-1}$  for 5-ASA, Cu(II) and Ni(II) complexes, respectively. The compounds induced detectable changes in the CD spectra of ct-DNA (B  $\rightarrow$  A structural transition, B  $\rightarrow$  C structural transition and stabilization of the right-handed B form, for mesalamine, Cu(II) and Ni(II) complexes, respectively). The competitive binding experiments with Hoechst 33258 indicated that 5-ASA and copper complex could interact as groove binders. Furthermore, Ni complex had no effect on the fluorescence intensity and peak position of MB-DNA system. Finally, the results obtained from experimental and molecular modeling showed that complexes bind to DNA via minor-groove binding.

**Keywords:** Cu(II) and Ni(II) complexes; ct-DNA; Groove-binding; Molecular modeling; Fluorescence quenching

\*Corresponding author. Email: [n.shahabadi@razi.ac.ir](mailto:n.shahabadi@razi.ac.ir)

## 1. Introduction

Studies on the interaction of transition metal complexes with DNA continue to attract attention due to their importance in design and development of synthetic restriction enzymes, chemotherapeutic drugs, and DNA footprinting agents. DNA is an important cellular receptor; many chemicals exert their antitumor effects by binding to DNA. Changing the replication of DNA and inhibiting the growth of the tumor cells, which is the basis of designing new and more efficient antitumor drugs and their effectiveness depends on the mode and affinity of the binding [1]. These complexes offer an opportunity to explore the effects of the central metal, the ligands and the coordination geometries on the binding event. By varying the ligands, it is possible to modify the mode of interaction of the complex with nucleic acids and facilitate individual applications. The application of octahedral complexes has permitted the targeting of specific DNA sites by matching the shape, symmetry, and functionality of the metal complex to that of the DNA target. There has also been increased interest in the study of metallo-intercalators, which play an important role in nucleic acid chemistry for applications such as footprinting, sequence-specific binding and reactions, new structural probes, and therapeutic agents [2].

Copper is a biologically relevant element, and many enzymes that depend on copper for their activity have been identified. Because of its biological relevance, a large number of copper(II) complexes have been synthesized and explored for their biological activities [3]. Artificial nucleases will provide important new tools for DNA manipulation to molecular biologists. For example, [bis(phenanthroline)copper(II)] is used in DNA footprinting experiments, which are important for the detailed study of DNA–protein interactions. The role of ternary copper(II) complexes in biological systems is well known. Recent reports have shown that amino acid/peptide based copper(II) complexes show efficient DNA cleavage activity by oxidative and hydrolytic pathways [4].

Nickel is an essential component in enzymes such as urease, carbon monoxide dehydrogenase, and hydrogenase. Recently, some results show potential of this platinum group element in antitumor studies [5]. Nickel complexes have been receiving much attention due to biological applicability, such as antiepileptic [6], anticonvulsant [7], antibacterial [8], antifungal [9], antimicrobial [10], and anticancer/antiproliferative [11] activities. Nickel complexes can inhibit the DNA-repair mechanism due to interfering with enzymes or proteins syntheses involved in DNA replication or DNA repair [12].

In our laboratory, we have focused our attention on designing improved drugs that target cellular DNA for understanding the mechanism of action at the molecular level and also investigating the effect of known drugs as anticancer agents. Therefore, we have previously shown that mesalamine (5-ASA) interacts with DNA via groove-binding mode [13].

In the present work, new copper(II) and nickel(II) complexes of mesalamine (5-ASA) drug were synthesized and characterized. In addition, the interaction of these complexes with DNA was studied using electronic absorption, fluorescence, circular dichroism (CD) spectroscopies, and viscosity measurements and was modeled by molecular docking. The aim was to check for differences between DNA interactions of 5-ASA and its copper and nickel complexes and show the effect of metal center on DNA binding. The results will be used to indicate the role of Ni(II) and Cu(II) ions in biological activity of mesalamine.

## 2. Experimental

### 2.1. Materials

Mesalamine, Hoechst 33258, calf thymus DNA (ct-DNA) and Tris-HCl were purchased from Sigma and nickel(II)/copper(II)-nitrate trihydrate, acetone, ethanol, and potassium hydroxide (KOH) were purchased from Merck. Experiments were carried out in Tris-HCl buffer at pH 7.4. The buffer solution was prepared from Tris-(hydroxymethyl)-amino-methane in double distilled water and hydrogen chloride, and pH was adjusted to 7.4. Stock solution of ct-DNA was prepared by dissolving about 2 mg of ct-DNA fibers in 2 mL Tris-HCl buffer (10 mM) by shaking gently and stored for 24 h at 4 °C and used within 5 days. The concentration of ct-DNA solution was expressed in monomer units, as determined by spectrophotometry at 260 nm using an extinction coefficient ( $\epsilon_p$ ) of  $6600 \text{ M}^{-1} \text{ cm}^{-1}$ . A solution of ct-DNA in the buffer gave a ratio of UV absorbance at 260 : 280 nm of  $\sim 1.8\text{--}1.9 : 1$ , indicating that the ct-DNA was sufficiently free from protein [14, 15]. Stock solutions of the complexes and 5-ASA were prepared by dissolving 0.81, 0.80, and 0.3 mg of the Cu/Ni complexes and 5-ASA, respectively, in 2.0 mL of Tris-HCl buffer (50 mM) (final concentration =  $10^{-3}$  M). Aliquots of the DNA solution were treated with 5-ASA and its Cu/Ni (II) complexes at several input molar ratios ( $r_i$ ), ( $r_i = [\text{DNA}]/[\text{5-ASA}]$  or  $[\text{M(II) complex}]$ ) at a constant complex concentration. It was reached to final volume of samples with Tris-HCl (50 mM) then incubated at 25 °C for 2 h.

### 2.2. Apparatus

The UV-vis spectra for ct-DNA-5-ASA and ct-DNA-complex interactions were obtained using an Agilent 8453 spectrophotometer. CD measurements were recorded on a JASCO (J-810) spectropolarimeter. Viscosity measurements were made using a viscosimeter (SCHOT AVS 450) thermostated at  $25 \pm 0.5$  °C by a constant temperature bath. Fluorescence measurements were carried out with a JASCO spectrofluorimeter (FP 6200). The mass spectra of complexes were recorded with Agilent Technology (HP) Model: 5973 Network Mass Selective Detector.

**2.2.1. Synthesis of nickel(II) complex of mesalamine.** To a solution of 5-ASA (0.50 g, 0.0033 mol) in ethanol-acetone (1 : 1) mixture (50 mL), 0.1 N KOH solution was added dropwise with stirring. The pasty precipitate was obtained at neutral pH. The precipitate was dissolved by addition of water to a clear solution (diluted to 85 mL). The stock solution was added dropwise to the solution of nickel(II)-nitrate trihydrate (0.48 g, 0.0016 mol) in water at room temperature. Sodium acetate or ammonia was added to complete precipitation. The precipitate was digested on a water bath at 80 °C for 2 h. The digested precipitate of the complex was filtered and washed with water and air-dried [16]. Anal. found (Calcd) for  $\text{C}_{14}\text{H}_{16}\text{N}_2\text{O}_8\text{Ni}$ : C% 43.8(42.15); H% 4.4(4.04); N% 7.9(7.02).

**2.2.2. Synthesis of copper(II) complex of mesalamine.** The copper complex of mesalamine was synthesized according to the above procedure in which copper(II) nitrate trihydrate was added to 5-ASA solution (copper(II)-nitrate trihydrate; 0.40 g, 0.0016 mol). Anal. found (Calcd) for  $\text{C}_{14}\text{H}_{16}\text{N}_2\text{O}_8\text{Cu}$ : C% 42.1(41.64); H% 4.3(3.99); N% 7.3(6.94).

### 2.3. Experimental procedures

**2.3.1. UV–vis absorption.** Absorbance spectra were recorded using an hp spectrophotometer (Agilent 8453) equipped with a thermostated bath (Huber polysat cc1). Absorbance experiments for interaction of 5-ASA and DNA were studied by keeping the 5-ASA concentration constant ( $3 \times 10^{-5}$  M) while varying the DNA concentration from 0 to  $9.1 \times 10^{-4}$  M ( $r_i = [\text{DNA}]/[\text{5-ASA}] = 0\text{--}18.2$ ). DNA interaction of Ni(II) and Cu(II) complexes was carried out by keeping the concentrations of the complexes constant ( $1 \times 10^{-4}$  and  $1.75 \times 10^{-4}$  M, respectively) while varying the DNA concentration from 0 to  $3.6 \times 10^{-3}$  and  $0\text{--}1.69 \times 10^{-3}$  M, respectively. Absorbance values were recorded after 2-h incubation of the solutions at 37 °C.

**2.3.2. Circular dichroism.** The effect of 5-ASA and its Cu/Ni (II) complexes on the conformation of secondary structure of ct-DNA was studied by keeping the concentration of ct-DNA constant ( $5 \times 10^{-5}$  M) in Tris–HCl buffer (50 mM) while varying the concentration of 5-ASA ( $r_i = [\text{drug}]/[\text{ct-DNA}] = 0\text{--}0.6$ ), Ni(II) complex ( $r_i = 0\text{--}0.9$ ), and Cu(II) complex ( $r_i = 0\text{--}2.8$ ). The spectra of the ct-DNA and those with the additives were monitored from 220 to 300 nm. CD spectra of ct-DNA in the presence and the absence of 5-ASA and its Cu/Ni (II) complexes were obtained using a JASCO spectropolarimeter (J-810) at 25 °C using 0.5 cm (1 mL) path length quartz cuvette.

**2.3.3. Viscosity.** In this study, a viscosimeter (SCHOT AVS 450) which was thermostated at 25 °C by a constant temperature bath was used. Flow time was measured with a digital stopwatch; the mean values of three replicated measurements were used to evaluate the viscosity  $\eta$  of the samples. DNA concentrations were constant ( $5.0 \times 10^{-5}$  M), and the  $r_i$  values are 0–0.6 for 5-ASA, Ni(II) complex and Cu(II) complex. The data are reported as  $(\eta/\eta^0)^{1/3}$  versus  $1/R$  ( $R = [\text{compound}]/[\text{DNA}]$  ratios) where  $\eta^0$  is the viscosity of the DNA solution alone,  $\eta = (t - t^0)/t^0$ ,  $t$  = sample flow time and  $t^0$  = the buffer flow time. The output of the instrument is flow time ( $t$ ).

**2.3.4. Fluorescence measurements.** Fluorescence intensities were measured using a JASCO spectrofluorimeter (FP 6200). In the competitive binding studies using Hoechst 33258 and methylene blue (MB), for 5-ASA, Cu(II) complex and Ni(II) complex,  $[\text{5-ASA}] = 0\text{--}2.7 \times 10^{-5}$  M,  $[\text{Hoechst}] = 5.0 \times 10^{-6}$  M and  $[\text{ct-DNA}] = 4.9 \times 10^{-6}$  M,  $[\text{Cu(II) complex}] = 0\text{--}6.1 \times 10^{-5}$  M,  $[\text{Hoechst}] = 5.0 \times 10^{-6}$  M and  $[\text{ct-DNA}] = 5.2 \times 10^{-4}$  M,  $[\text{Ni(II) complex}] = 0\text{--}5.6 \times 10^{-5}$  M,  $[\text{MB}] = 9.0 \times 10^{-6}$  M and  $[\text{ct-DNA}] = 1.06 \times 10^{-4}$  M, respectively. The excitation wavelengths were at 340 nm, and emissions were observed between 360 and 600 nm.

**2.3.5. Molecular docking study.** MGL tools 1.5.6 with AutoGrid4 and AutoDock4 [17, 18] were employed to set up and carry out blind docking calculations between the complexes and DNA sequence. ct-DNA sequence d(CGCGAATTCGCG)2 dodecamer (PDB ID: 1BNA) was retrieved from the Protein Data Bank. Receptor (DNA) and ligand (complex) files were prepared using AutoDock Tools. The Cu complex and Ni complex systems were enclosed in a box with grid points in  $x \times y \times z$  directions, ( $56 \times 66 \times 112$ ) and

( $54 \times 62 \times 112$ ), respectively, and a grid spacing of  $0.375 \text{ \AA}$ . Lamarckian genetic algorithms, as implemented in AutoDock, were employed to perform docking calculations. All other parameters were default settings. For each of the docking cases, the lowest energy docked conformation, according to the Autodock scoring function, was selected as the binding mode. The amounts of independent docking runs performed for each docking simulation was set to 200. Cluster analysis was performed on the docked results using a root mean square tolerance of  $0.5 \text{ \AA}$ , and the initial coordinates of the ligand were used as the reference structure. The structures of molecules were optimized using HyperChem (HyperCube Inc., Gainesville, FL). All the molecular images and animations were produced using VMD [19].

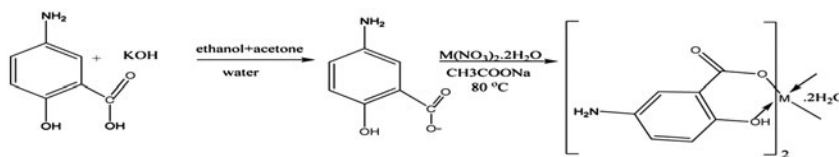
### 3. Results and discussion

#### 3.1. Synthesis of copper and nickel complexes

The synthetic route of the synthesis of M(II) complexes from the reaction of  $[M(\text{NO}_3)_2 \cdot n\text{H}_2\text{O}]$  and 5-ASA ligand is shown in scheme 1.

#### 3.2. Characterization of the complexes

**3.2.1. Theoretical method.** Calculations on the structures of the complexes were performed by the appropriate theoretical method. The calculations were performed by Spartan'10 package [20]. The structures of the complexes were obtained by PM6 method [21]. The suggested chemical formula (figure 1) is  $[M(5\text{-ASA})_2(\text{H}_2\text{O})_2]$ . The central metal of the octahedron is surrounded by two phenol oxygens of 5-ASA molecules, two water molecules, and two carboxylate oxygens of 5-ASA molecules. The carboxylate and the phenol oxygens of the two 5-ASA molecules define the equatorial positions, whereas the two water molecules occupy the axial ones. The axial M–O bond distances of  $2.555 \text{ \AA}$  ( $\text{O}_7$  and  $\text{O}_8$ ) are significantly longer than the equatorial M–O bonds of  $1.856 \text{ \AA}$  ( $\text{O}_1$  and  $\text{O}_4$ ) and  $1.914 \text{ \AA}$  ( $\text{O}_3$  and  $\text{O}_6$ ). The axial angle  $\text{O}_7\text{--M--O}_8$  is  $179.12^\circ$ , where the equatorial  $\text{O}_3\text{--M--O}_4$  is  $179.48^\circ$ . The equatorial O–M–O bond angles are  $92.11^\circ$  for  $\text{O}_1\text{--M--O}_3$  and  $\text{O}_4\text{--M--O}_6$ . The calculated structure with the atom numbering scheme of the complex is shown in figure 1. The average O–M–O bond angles are in accord with those known for a reported nickel (II) distorted octahedral geometry [22]. Therefore, two 5-ASA molecules and two water molecules are directly involved in coordination.



Scheme 1. Chemical reactions in the synthesis of copper(II) and nickel(II) mesalamine complexes.

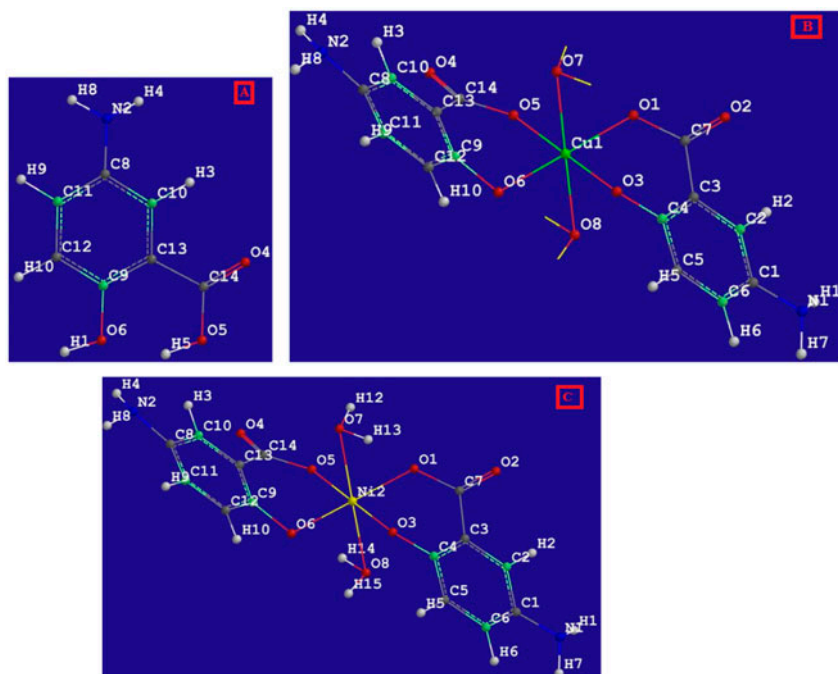


Figure 1. The structures of (a) 5-ASA, (b) copper complex, and (c) nickel complex.

**3.2.2. Spectroscopic methods.** The complexes were characterized by UV-vis, IR, and mass spectra. The electronic spectra of the ligand and the complexes were recorded in Tris-HCl buffer at room temperature. In comparison with the free ligand spectrum, the nickel complex spectrum has characteristic features as shown in figure 2(A). The electronic absorption spectrum of 5-ASA exhibits an absorption at 220 nm assigned to  $\pi$ - $\pi^*$  transition. In nickel(II) complex, a new absorption at 326 nm is assigned to charge transfer (LMCT) in the complex. These features prove that the complex has been prepared. The electronic

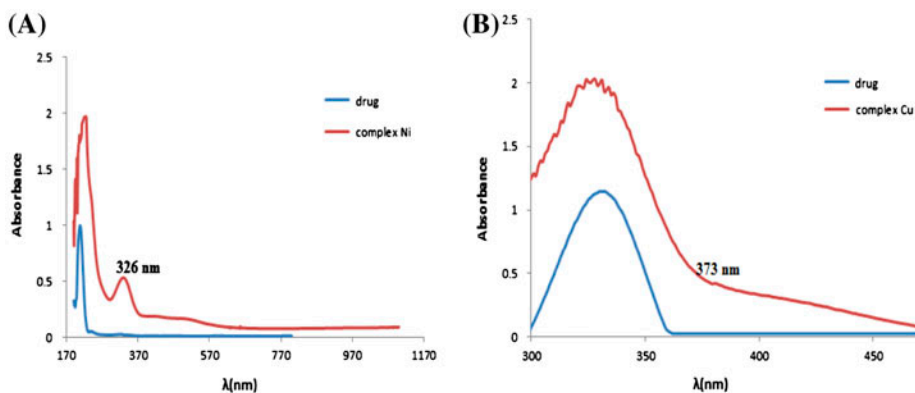


Figure 2. (A) UV spectra of 5-ASA ( $1 \times 10^{-6}$  M) and nickel complex ( $1 \times 10^{-6}$  M) in Tris-HCl buffer. (B) UV spectra of 5-ASA ( $8 \times 10^{-5}$  M) and copper complex ( $8 \times 10^{-5}$  M) in Tris-HCl buffer.

Table 1. IR data for the free ligand and its copper(II)/nickel(II) complexes (in  $\text{cm}^{-1}$ ).

Compound	$\nu(\text{C}=\text{O})_{\text{COOH}}$	$\nu(\text{M}-\text{O})$	$\nu(\text{C}-\text{H})_{\text{aromatic}}$
5-ASA	1652	–	685–809
Cu(II)	1605	539	684–809
Ni(II)	1633	544.8	685–900

absorption spectrum of 5-ASA and its copper(II) complex are shown in figure 2(B). The new absorption around 373 nm is assigned to charge transfer (LMCT) of the complex.

For interpretation of the IR data, the spectra were divided into two groups. The absorption bands at  $4000\text{--}600\text{ cm}^{-1}$  belong to absorptions of the ligand. The absorption bands in the far IR below  $600\text{ cm}^{-1}$  characterize the ligand–metal bonding. IR spectra of 5-ASA and its copper complex are shown in figure S1(A) and (B) [see online supplemental material at <http://dx.doi.org/10.1080/00958972.2015.1078897>] and spectral data are collected in table 1. Absorption bands of 5-ASA in the IR spectrum are affected by the coordination. The characteristic band of  $\nu(\text{C}=\text{O})$  is at  $1605\text{ cm}^{-1}$ . In the spectrum of the free ligand, it was found at  $1652\text{ cm}^{-1}$ , shifted approximately  $47\text{ cm}^{-1}$  upon coordination. The spectrum of copper(II) complex exhibits a new absorption band at  $539\text{ cm}^{-1}$  [23]. Also for the nickel complex [figure S1(C)], the characteristic band of  $\nu(\text{C}=\text{O})$  is at  $1633\text{ cm}^{-1}$ . The frequency of the 5-ASA absorption shifted  $28\text{ cm}^{-1}$  upon coordination in comparison with the spectrum of free 5-ASA. The spectrum of nickel(II) complex has a new absorption at  $545\text{ cm}^{-1}$  which was assigned to M–O stretching vibration [22].

Mass spectrum of the ligand shows the molecular ion peak at  $m/z$  153. The copper complex ( $\text{C}_{14}\text{H}_{16}\text{CuN}_2\text{O}_8$ ) shows the molecular ion peak ( $M + 1$ ) at  $m/z$  405 [figure S2(A)]. In addition, a peak at  $m/z$  368 is due to the ionization of two water molecules. The nickel complex ( $\text{C}_{14}\text{H}_{16}\text{NiN}_2\text{O}_8$ ) shows the molecular ion peak ( $M + 1$ ) at  $m/z$  400 [figure S2(B)] and the base peak at  $m/z$  363 which is due to ionization of two water molecules. The data confirm the stoichiometry of the metal complexes as  $[\text{ML}_2(\text{H}_2\text{O})_2]$  type. The coordination of water was ascertained by CHN analysis.

### 3.3. DNA interaction studies

**3.3.1. Absorption studies.** UV–vis absorption measurement is a simple but effective method in detecting complex formation [24]. In general, when a small molecule interacts with DNA and forms a new complex, changes in absorbance and in the position of the band occur [25]. If the binding mode is intercalation, the  $\pi^*$  orbital of the intercalated molecule can couple with the  $\pi$  orbital of the DNA base pairs, thus, decreasing the  $\pi \rightarrow \pi^*$  transition energy and resulting in bathochromism. On the other hand, the coupling  $\pi$  orbital is partially filled by electrons, thus decreasing the transition probabilities and concomitantly resulting in hypochromism [26]. In general, hyperchromism and hypochromism concern the double helix structure of DNA; hyperchromism means the breakage of the secondary structure of DNA [27] and hypochromism results from the contraction of DNA in the helix axis, as well as from the conformational change of DNA [28]. The experiment was carried out for a fixed concentration of free 5-ASA ( $5 \times 10^{-5}\text{ M}$ ) with increasing concentrations of ct-DNA ( $0\text{--}9.1 \times 10^{-4}\text{ M}$ ) [figure 3(A)]. In the presence of ct-DNA, the UV spectrum shows a decrease in the peak intensity at 331 nm. No red shift was observed in the UV spectra, which indicates that the binding mode is not intercalation and the hypochromism



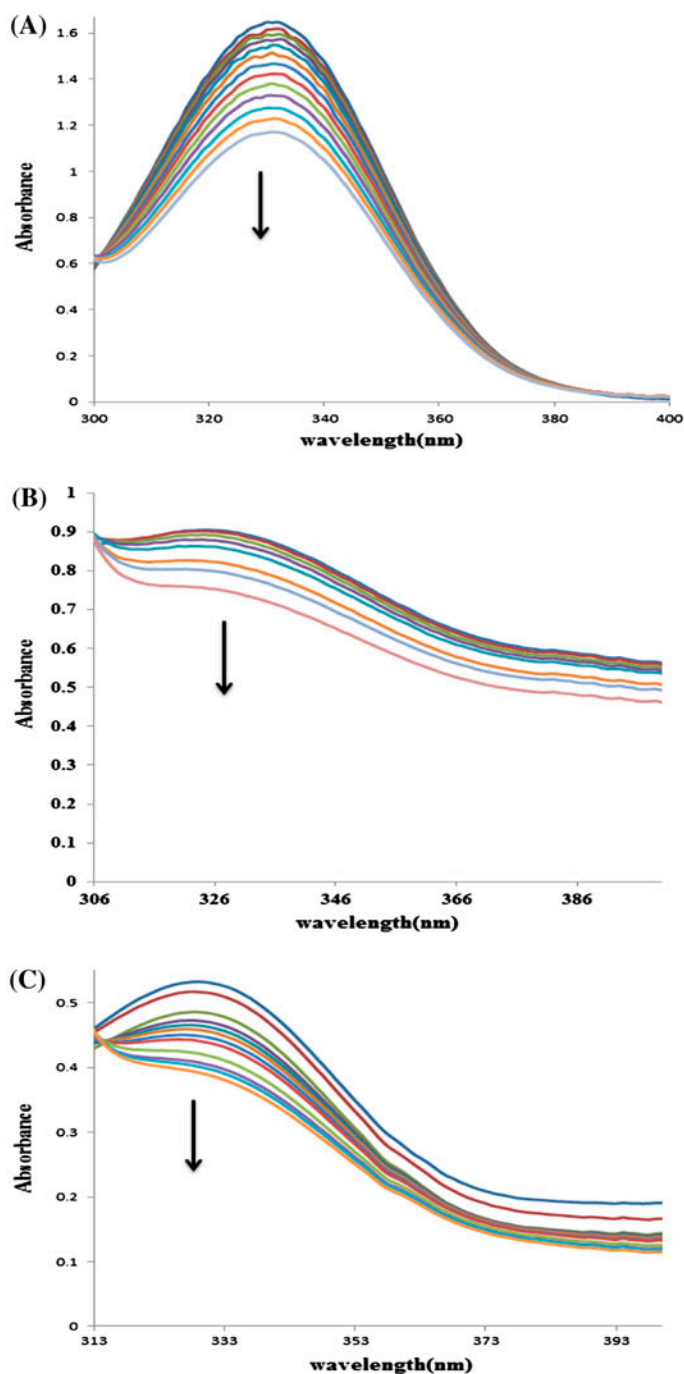


Figure 3. (A) UV absorption spectra of 5-ASA in the presence of different concentrations of ct-DNA at pH 7.4 and room temperature.  $[5\text{-ASA}] = 5 \times 10^{-5}$  M and  $[\text{ct-DNA}] = 0.0\text{--}9.1 \times 10^{-4}$  M. (B) UV absorption spectra of copper complex in the presence of different concentrations of ct-DNA at pH 7.4 and room temperature.  $[\text{Complex}] = 1.75 \times 10^{-5}$  M and  $[\text{ct-DNA}] = 0.0\text{--}1.69 \times 10^{-3}$  M. (C) UV absorption spectra of nickel complex in the presence of different concentrations of ct-DNA at pH 7.4 and room temperature.  $[\text{Complex}] = 1 \times 10^{-4}$  M and  $[\text{ct-DNA}] = 0.0\text{--}3.6 \times 10^{-3}$  M.

indicates that the binding mode of 5-ASA to DNA might be groove binding [29]. The intrinsic binding constant,  $K_b$ , for 5-ASA was calculated from Wolfe–Shimmer equation (1),

$$\frac{[\text{DNA}]}{(\varepsilon_A - \varepsilon_f)} = \frac{[\text{DNA}]}{(\varepsilon_b - \varepsilon_f)} + \frac{1}{K_b(\varepsilon_b - \varepsilon_f)} \quad (1)$$

where [DNA] was the concentration of ct-DNA,  $\varepsilon_a$ ,  $\varepsilon_f$ , and  $\varepsilon_b$  corresponded to the apparent extinction coefficient, the extinction coefficient for the free compound and its fully ct-DNA-bound combination, respectively. In the plots of  $[\text{ct-DNA}]/(\varepsilon_a - \varepsilon_f)$  versus [ct-DNA],  $K_b$  was derived as the ratio of the slope to y intercept. The ct-DNA binding constant is  $1.27 \times 10^3 \text{ M}^{-1}$ , comparable to groove-binding drugs such as 2-imidazolidinethione and levetiracetam with  $K_b = 1.4 \times 10^3$  and  $4.9(\pm 0.2) \times 10^3 \text{ M}^{-1}$ , respectively [29, 30].

The experiment was carried out for a fixed concentration of copper complex ( $1.75 \times 10^{-5} \text{ M}$ ) with increasing concentrations of ct-DNA ( $0$ – $1.69 \times 10^{-3} \text{ M}$ ) [figure 3(B)]. With the addition of ct-DNA, UV spectrum shows a decrease in peak intensity at 325 nm. Also the experiment was carried out for a fixed concentration of nickel complex ( $1.0 \times 10^{-4} \text{ M}$ ) with increasing concentrations of ct-DNA ( $0$ – $3.6 \times 10^{-3} \text{ M}$ ) [figure 3(C)]. With the addition of ct-DNA, UV spectrum of the complex showed decrease in the peak intensity at 328 nm. No red shift was observed in the UV spectra, and these hypochromism changes indicate that the interaction of copper and nickel complexes to DNA might be groove binding. The ct-DNA binding constants with copper and nickel complexes are  $2 \times 10^4$  and  $1.2 \times 10^4 \text{ M}^{-1}$ , respectively.

Finally, the results show that the binding constants of the nickel complex ( $1.2 \times 10^4 \text{ M}^{-1}$ ) and copper complex ( $2 \times 10^4 \text{ M}^{-1}$ ) are greater than that for 5-ASA ( $1.27 \times 10^3 \text{ M}^{-1}$ ). Therefore, the DNA-binding affinity of the complexes is higher than the drug.

**3.3.2. CD spectral studies.** CD spectroscopy is widely used to characterize the conformation of biological molecules. The differential absorption of right- and left-handed polarized light arises from chirality of the chromophore. For DNA, the individual nucleotides are asymmetrical, and the CD signal provides a convenient way to assess changes in the conformational state of oligonucleotides and polymers as a function of temperature, pressure, ionic strength, and other parameters. Because of the dependence of the CD signal on the symmetry of the molecular environment of the chromophore, DNA exhibits CD signals that are characteristic of various conformational states. The A-, B-, and Z-conformations of DNA exhibit distinct CD spectra, and it is often possible to monitor directly the presence of a particular conformation. Indeed, CD is one of the most powerful techniques for investigating the properties of the helix produced by ligand binding. The CD spectrum of ct-DNA consists of a positive band at 275 nm due to base stacking and a negative band at 245 nm due to helicity, which is characteristic of DNA in right-handed B form, in the ultraviolet region [31]. CD spectral techniques may give us information on how the helicity of the ct-DNA chain influences the electronic transitions of a bound drug. The effect of 5-ASA on the conformation of the secondary structure of ct-DNA was investigated by keeping the concentration of DNA constant ( $8 \times 10^{-5} \text{ M}$ ) while varying the drug concentration ( $r_i = [\text{Drug}]/[\text{ct-DNA}] = 0$ – $0.6$ ). As shown in figure 4(A) (the CD spectrum of ct-DNA in

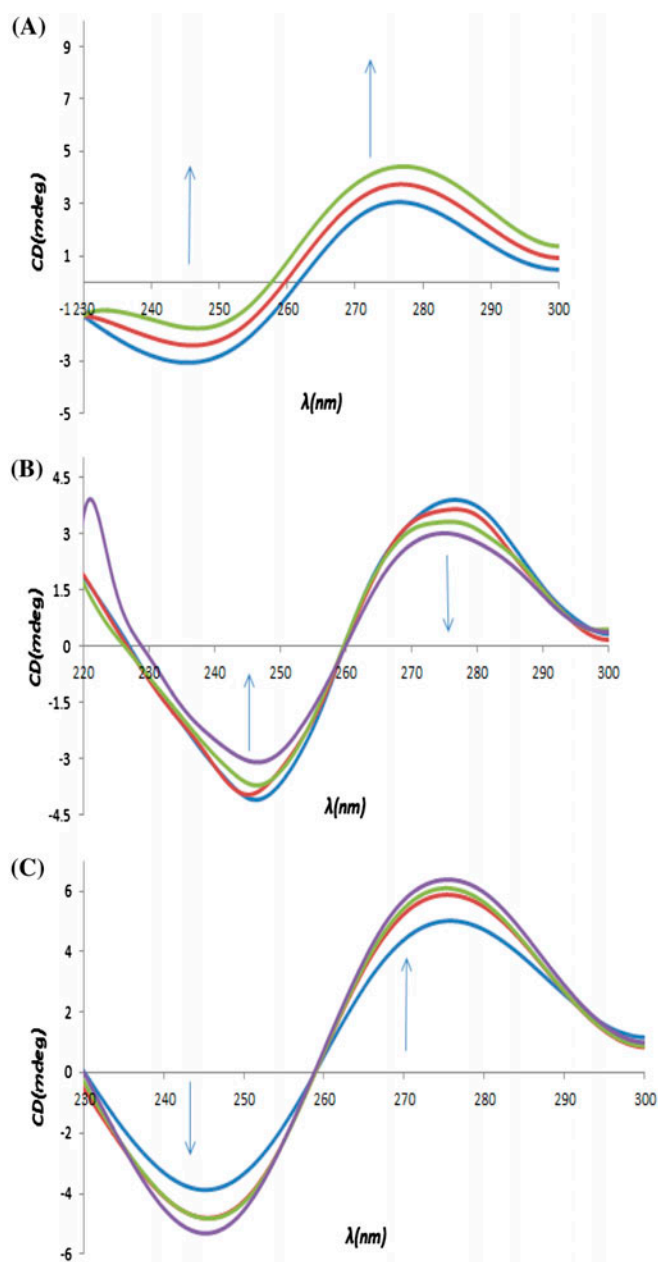


Figure 4. (A) CD spectra of ct-DNA in the absence (blue line) and the presence of 5-ASA ( $r_1 = [5\text{-ASA}]/[\text{ct-DNA}] = 0\text{--}0.6$ ). (B) CD spectra of ct-DNA in the absence and the presence of copper complex ( $r_1 = [\text{Complex}]/[\text{ct-DNA}] = 0\text{--}2.88$ ). (C) CD spectra of ct-DNA in the absence and the presence of nickel complex ( $r_1 = [\text{Complex}]/[\text{ct-DNA}] = 0\text{--}0.9$ ) (see <http://dx.doi.org/10.1080/00958972.2015.1078897> for color version).

the presence of 5-ASA), the intensity of the positive peak increased while the intensity of the negative peak decreased [15], reflecting a shift from B-like ct-DNA structure toward one with some contributions from an A-like conformation [29, 32].

As shown in figure 4(B) in the presence of the copper complex, CD spectra of DNA decreased in the positive and negative bands due to a transition from a more B-like to a more C-like structure.

The CD spectrum of ct-DNA in the presence of the nickel complex showed that both the positive and negative peak intensities of the CD spectra of DNA increased. The changes in the CD spectra in the presence of nickel complex show stabilization of the right-handed B form of ct-DNA [figure 4(C)].

**3.3.3. Viscosity measurements.** Hydrodynamic methods, such as the determination of viscosity, which is sensitive to the change of length of DNA, may be the most effective means studying the binding mode of complexes to DNA in the absence of X-ray crystallographic or NMR structural data [33]. A classical intercalation binding requires the space of adjacent base pairs to be large enough to accommodate the bound small molecules and to elongate the double helix, resulting in an increase of ct-DNA viscosity [34]. In contrast, there is little effect on the viscosity of DNA if electrostatic or groove binding occurs [35]. The values of the relative specific viscosities for 5-ASA, copper complex, and nickel complex ( $\eta/\eta_0$ )<sup>1/3</sup> plotted against 1/R ( $R = [\text{Complex}]/[\text{ct-DNA}]$ ) are shown in figure 5, respectively. The viscosity data in three cases show little changes on the viscosity of ct-DNA, suggesting that 5-ASA, copper complex, and nickel complex bind to ct-DNA by groove binding.

**3.3.4. Fluorescence spectroscopic studies.** One approach to study the binding mechanism between ct-DNA-drug is fluorescence quenching technique. Fluorescence quenching refers to any process which decreases the fluorescence intensity of a sample [36]. To clarify quenching mechanism, fluorescence quenching spectra were measured at different temperatures [37]. Luminescence was observed for 5-ASA and nickel complex in the absence and presence of increasing amounts of ct-DNA. The decrease in the emission maxima of 5-ASA and Ni(II) complex after each addition of ct-DNA indicated interaction between ct-DNA and 5-ASA and its nickel complex [figure S3(A) and (B), respectively]. Fluorescence quenching is described by the Stern–Volmer equation,

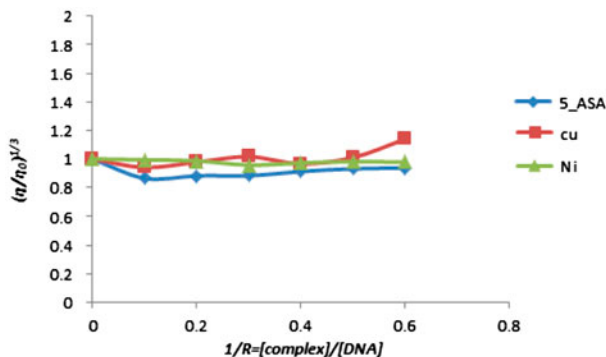


Figure 5. Effects of increasing amounts of 5-ASA, copper and nickel complexes on the relative viscosity of ct-DNA at 298 K and pH 7.4. [ct-DNA] =  $5 \times 10^{-5}$  M ( $r_i = [\text{Compound}]/[\text{ct-DNA}]$ ).

Table 2. The quenching constants of 5-ASA and its nickel complex by ct-DNA at different temperatures.

Compound	$T$ (K)	$R^2$	$K_q$ ( $M^{-1}$ ) $\times 10^{11}$	$K_{sv}$ ( $M^{-1}$ ) $\times 10^3$
5-ASA	283	0.99	0.1417	0.1417
	298	0.99	0.1396	0.1396
	310	0.97	0.124	0.124
Nickel complex	283	0.99	0.140	0.140
	298	0.99	0.120	0.120
	310	0.99	0.113	0.113

$$\frac{F_0}{F} = 1 + K_q \tau_0 [Q] = 1 + K_{sv} [Q] \quad (2)$$

where  $F_0$  and  $F$  represent the fluorescence intensities in the absence and in the presence of quencher, respectively.  $K_q$  is the fluorophore quenching rate constant,  $K_{sv}$  is quenching constant,  $\tau_0$  is the lifetime of the fluorophore in the absence of a quencher ( $\tau_0 = 10^{-8}$  s), and  $[Q]$  is the concentration of quencher [38]. The results in table 2 indicate that the probable quenching mechanism of 5-ASA and the nickel complex by ct-DNA involve static quenching because  $K_{sv}$  decreases with increasing temperature [39]. Additionally, the Stern–Volmer quenching constants,  $K_{sv}$ , were determined to be  $0.139 \times 10^3$  and  $0.120 \times 10^3 M^{-1}$ , respectively, at 25 °C, lower than classical intercalators like nile blue 2-tert-butyl-4-methylphenol ( $1.3 \times 10^4 M^{-1}$ ) showing the relatively lower affinity of the studied 5-ASA and the nickel complex, in agreement with the binding strength difference between the groove binding and intercalation [40].

3.3.4.1. *Equilibrium binding titration.* The binding constant ( $K_f$ ) and the binding stoichiometry ( $n$ ) for the complex formation between 5-ASA and nickel complex and ct-DNA were measured according to the method described by Hu *et al.* [equation (3)] [41],

$$\text{Log}(F_0 - F)/F = \text{log } K_f + n \text{ log}[Q] \quad (3)$$

In this equation,  $F_0$  and  $F$  are the fluorescence intensities of the fluorophore in the absence and in the presence of different concentrations of quencher, respectively. The values of  $K_f$  and  $n$  are shown in table 3.

3.3.4.2. *Thermodynamic parameters of DNA binding.* Data obtained from enthalpy changes ( $\Delta H$ ) and entropy changes ( $\Delta S$ ), the model of interaction between drug and biomolecule can be concluded [42]: (1)  $\Delta H > 0$  and  $\Delta S > 0$ , hydrophobic forces; (2)  $\Delta H < 0$  and

Table 3. Binding constants ( $K_f$ ) and the number of binding sites ( $n$ ) of the DNA–5-ASA and DNA–Ni(II) complex.

Compound	$T$ (K)	$n$	$\text{Log } K_f$	$K_f \times 10^3$	$R^2$
5-ASA	283	1.28	3.88	7.585	0.99
	293	1.09	2.37	0.234	0.99
	310	0.99	2.04	0.109	0.97
Nickel complex	283	1.09	2.35	0.223	0.99
	293	1.45	2.07	0.117	0.99
	310	1.58	2.36	0.229	0.99

$\Delta S < 0$ , van der Waals interactions and hydrogen bonds; (3)  $\Delta H < 0$  and  $\Delta S > 0$ , electrostatic interactions [43].  $\Delta H$  and  $\Delta S$  were obtained from the slope and intercept of the linear plot based on  $\ln K$  versus  $1/T$  [figure S4(A) and (B)]. The values of  $\Delta H$ ,  $\Delta S$ , and  $\Delta G$  between 5-ASA and nickel complex with ct-DNA are listed in table 4. It can be seen that the negative values of  $\Delta G$  revealed the interaction process is spontaneous, while the negative  $\Delta H$  and  $\Delta S$  values indicated that hydrogen bond and van der Waals forces play main roles in the binding of 5-ASA to ct-DNA. According to the thermodynamic data, the formation of the ct-DNA–5-ASA complex is enthalpy favored while it is entropy disfavored. The complex formation results in a more ordered state, possibly due to the freezing of the motional freedom of both the 5-ASA and ct-DNA molecules. For nickel complex, the positive  $\Delta H$  and  $\Delta S$  values indicated that hydrophobic forces play main roles in the binding of nickel complex to ct-DNA.

Luminescence was observed for copper complex in the absence and the presence of increasing amounts of ct-DNA and the decrease in the emission maxima of copper complex after each addition of ct-DNA indicated the interaction between copper complex and ct-DNA. The decrease in the emission maxima of copper complex after each addition of ct-DNA is shown in figure 6 which causes a strong fluorescence quenching at 498 nm, and the appearance of an isosbestic point at 468 nm indicates the formation of a complex [44].

### 3.3.5. Calculation of thermodynamic parameters of Cu-DNA binding using spectrophotometry.

The absorbance measurements were performed by keeping the copper complex concentration constant ( $1.75 \times 10^{-5}$  M) while varying the ct-DNA concentration from 0.0 to  $1.69 \times 10^{-3}$  M. Experiments were measured at three temperatures (300, 308, and 319 K), and the spectra were recorded from 300 to 420 nm. With the addition of ct-DNA, UV spectra show decrease in the peak intensity at 323 nm. The intrinsic binding constant,  $K_b$ , for complex was calculated from Wolfe–Shimmer equation (1). The ct-DNA binding constants for three temperatures (300, 308, and 319 K) are  $1.42 \times 10^3$ ,  $1.50 \times 10^3$  and  $1.75 \times 10^3$  M<sup>-1</sup>, respectively.

$\Delta H$  and  $\Delta S$  were obtained from the slope and intercept of the linear plot based on  $\ln K$  versus  $1/T$  (figure S5). The values of  $\Delta H$ ,  $\Delta S$ , and  $\Delta G$  between copper complex with ct-DNA are listed in table 4. The positive value of  $\Delta S$  was evidence for hydrophobic interaction. The positive value of  $\Delta H$  showed that the binding process was mainly enthalpy driven by means of hydrogen bonds. So both hydrophobic interaction and hydrogen bonds might play roles in the binding of the copper complex to DNA. This result was in good accord with the information coming from the molecular modeling [45].

Table 4. Thermodynamic parameters for the bindings of 5-ASA, Ni(II) complex and Cu(II) complex to ct-DNA.

Compound	<i>T</i> (K)	$\Delta G$ (kJ mol <sup>-1</sup> )	$\Delta H$ (kJ mol <sup>-1</sup> )	$\Delta S$ (J mol <sup>-1</sup> K <sup>-1</sup> )
5-ASA	283	-15.79	-55.22	-139.32
	293	-13.70		
	310	-12.03		
Nickel complex	283	-12.95	63.75	271.04
	293	-17.01		
	310	-20.26		
Copper complex	300	-18.08	8.256	87.80
	308	-18.78		
	319	-19.75		

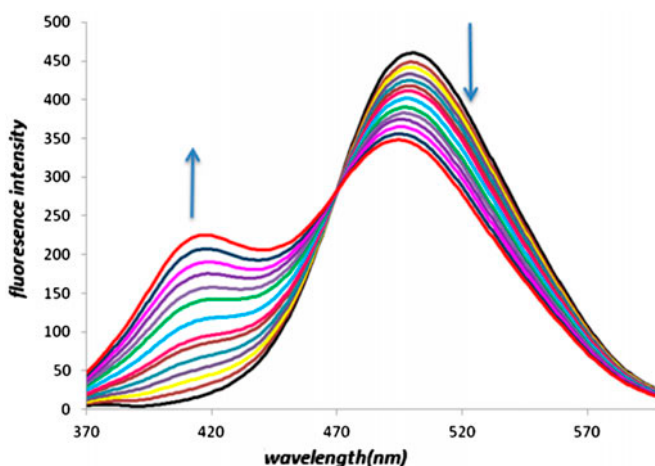


Figure 6. The influence of ct-DNA concentration on the fluorescence intensity of copper complex. Conditions: [complex] =  $5 \times 10^{-3}$  M; [ct-DNA] = 0– $3.06 \times 10^{-3}$  M.

**3.3.6. Competitive binding studies with Hoechst 33258.** To investigate the mode of 5-ASA and copper complex binding to ct-DNA, competitive binding experiments were performed. Hoechst 33258 binds strongly to the minor groove of double-stranded B-DNA with specificity for AT-rich sequences [46]. The interaction of Hoechst 33258 with DNA in Tris-HCl buffer (pH 7.4) was characterized by the fluorescence spectra. The 5-ASA was added fixed to amounts of the Hoechst 33258 and DNA ( $5 \times 10^{-6}$  and  $1.2 \times 10^{-4}$  M, respectively), and the copper complex was added fixed to amounts of the Hoechst 33258 and DNA ( $5 \times 10^{-6}$  and  $2.12 \times 10^{-4}$  M, respectively). Luminescence was observed for 5-ASA and copper complex in the absence and the presence of increasing amounts of ct-DNA. Fluorescence emission spectra are enhanced by increasing the DNA concentration [47]. With the addition of 5-ASA and copper complex to a solution of Hoechst-DNA, some Hoechst molecules were released into solution after an exchange with the 5-ASA and copper complex and resulted in fluorescence quenching [figure 7(A) and (B), respectively]. This supported the view that 5-ASA and copper complex could interact as minor-groove binders.

**3.3.7. Competitive binding between MB and nickel complex for DNA.** MB is the most widely used photosensitizing agent and alternative to ethidium bromide. The exact mode of binding of MB to DNA duplex is unknown, but its ionic interaction with negatively charged backbone  $\text{PO}_2$  groups can cause photo-oxidative damage generating singlet oxygen through a triplet-triplet energy transfer from the photoexcited dye to molecular oxygen. In the case of MB binding to DNA with alternating G-C base sequence, the spectroscopic data clearly indicated intercalation of the planar heterocyclic MB between neighboring base pairs, whereas in the case of binding to DNA with alternating base sequences, minor-groove binding is assumed to be the predominant binding mode. The planar heterocyclic dye is expected to stabilize its binding to DNA through favorable stacking interactions with its adjacent base pairs [48]. The experiment was performed by addition of the nickel complex to DNA solution which was pretreated with MB as a fluorescence probe (figure 8). The

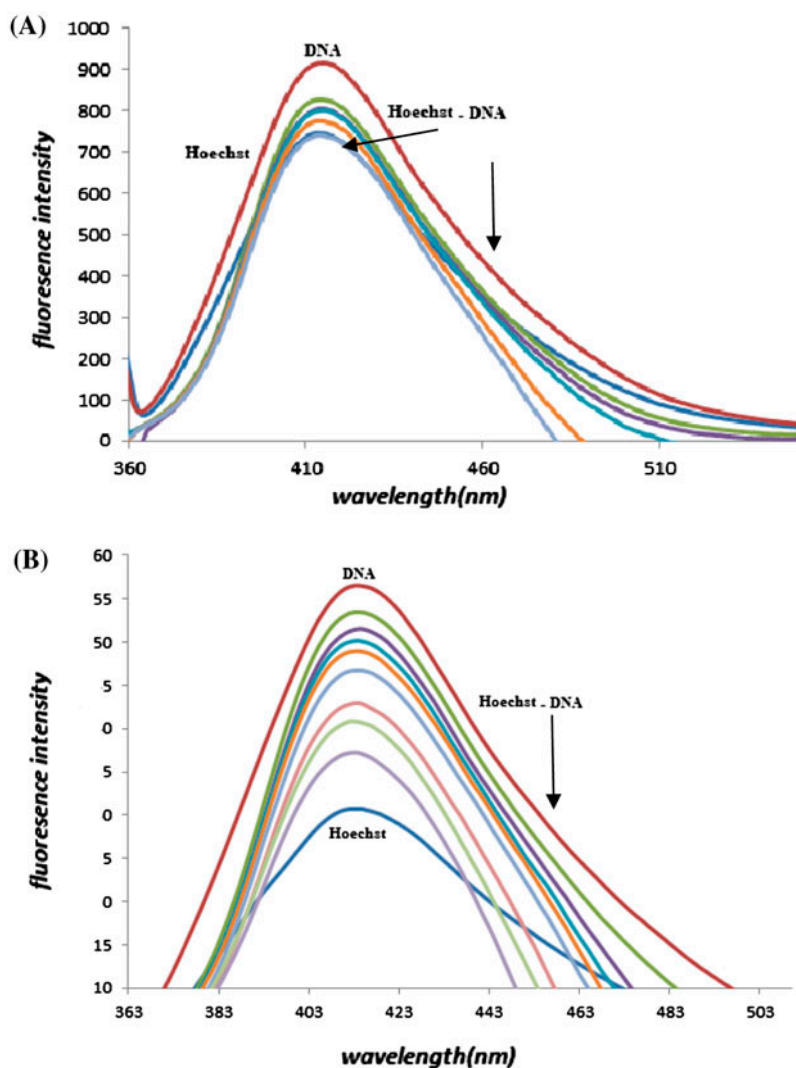


Figure 7. (A) Emission spectra of the Hoechst-DNA complex in the presence of increasing amounts of 5-ASA. (B) Emission spectra of the Hoechst-DNA complex in the presence of increasing amounts of copper(II) complex.

nickel complex was added to fixed amounts of MB and DNA ( $9 \times 10^{-6}$  and  $1.06 \times 10^{-4}$  M, respectively), and its effect on the emission intensity was measured. There is no change in the fluorescence intensity of the DNA-MB mixture upon adding the complex. This result is due to not releasing MB molecules from DNA-MB complex.

**3.3.8. Molecular docking studies on the interaction mechanism of complexes with DNA.** Molecular models were built to discuss the binding modes by docking using Auto-dock program for the interactions of molecules with multiple ct-DNA fragments [49]. The docking programs can be considered as computational filters to reduce labor and cost



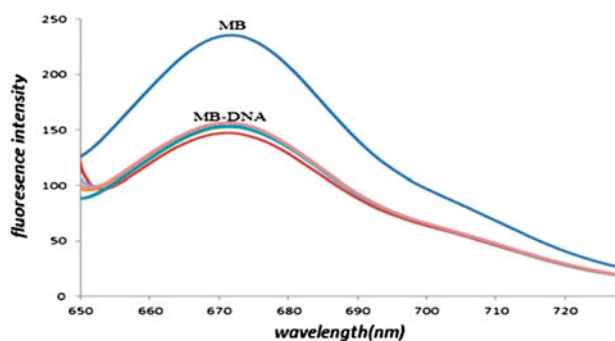


Figure 8. Emission spectra of the MB–DNA complex in the presence of increasing amounts of nickel(II) complex.

needed for the development of effective medicinal compounds when used prior to experimental screening. They can help in better understanding of bioactivity mechanisms when used after experimental screening [50]. Docking is important in the study of various properties associated with protein–ligand interactions such as binding energy, geometry complementarily, electron distribution, hydrogen bond donor acceptor properties, hydrophobicity, and polarizability [51]. In this study, docking was carried out to complement the experimental data. Using optimal energy, the complexes inserted into the minor grooves (figure 9) of DNA fragments and hydrophobic forces play main roles in the binding. There are hydrophobic contacts between C2 and C3 with DG2 and DG22, between C12 and C13 with DA5 and DC21 for copper complex and for Ni complex, and there are hydrophobic contacts between C2 and C3 with DG4, DG22 and also between C12 and C13 with DG5, DG6 (figure S6). There were hydrogen bonds between hydrogens of the copper complex with O<sub>4'</sub> of DG-22, and hydrogens of the nickel complex with O<sub>4'</sub> of DG-22 and N<sub>3</sub> of DG-22 (figure S7). These observations are further supported by hydrogen bonding interactions involving the energy-minimized docked poses of the DNA duplex with the complexes, as shown in table 5 [51]. This indicated again that hydrogen bonds played an important role in the binding of the complexes to DNA. Therefore, the results obtained from the molecular

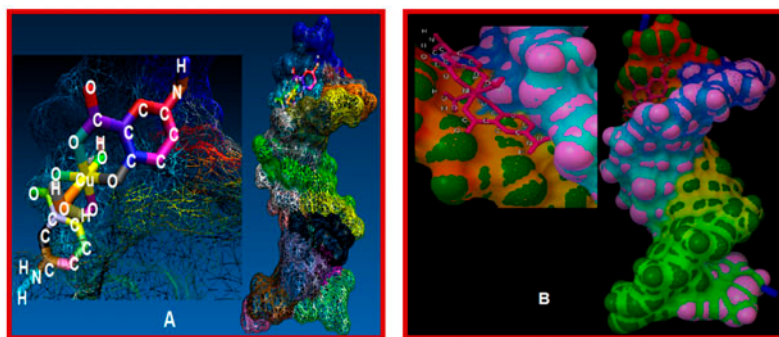


Figure 9. Molecular docking perspective of (A) the Cu(II) complex and (B) Ni(II) complex with the minor-groove side of DNA.

Table 5. Hydrogen bonding interactions involving the energy-minimized docked poses of DNA with the complexes.

Acceptor group (Y-H)	Donor group Z	Distance (Å)
O <sub>4</sub> -DG-22	H (Cu complex)	1.97
O <sub>4</sub> -DG-22	H (Ni complex)	1.91
N <sub>3</sub> -DG-22	H (Ni complex)	3.55

modeling correlates with our experimental results. From the docking simulation, the free energy change of binding ( $\Delta G$ ) for the copper complex was  $-34.5 \text{ kJ mol}^{-1}$  and for the nickel complex was  $-32.5 \text{ kJ mol}^{-1}$  compared to UV-vis absorption studies of  $18.2 \text{ kJ mol}^{-1}$  and  $23.17 \text{ kJ mol}^{-1}$  for Cu(II) and Ni(II) complexes, respectively. These imply good binding affinity between the complexes and DNA. The apparent mismatches in the free energy changes could be due to the exclusion of solvent.

#### 4. Conclusion

In this work, Cu(II) and Ni(II) complexes of mesalamine (5-ASA) were synthesized in order to improve water solubility of the complexes and influence better diffusion through membranes. Different instrumental methods were used to compare the interaction mechanisms of mesalamine and its metal complexes with ct-DNA. The results suggest that mesalamine and its metal complexes interact with DNA via groove binding as supported by: In absorption spectrum, the absorption intensity of 5-ASA, Cu(II) complex, and Ni(II) complex increased (hypochromism) after the addition of DNA, which indicated the interactions between DNA and 5-ASA and its complexes. The intrinsic binding constants ( $K_b = 1.27 \times 10^3$ ,  $2 \times 10^4$  and  $1.2 \times 10^4 \text{ M}^{-1}$ ) are more in keeping with groove binding with DNA. The relative viscosity of DNA solutions show little change with increasing concentrations of 5-ASA and metal complexes which is ascribed to groove binding of the drug and its complexes. Conformational changes show little or no perturbations on the base stacking and helicity bands, indicating that 5-ASA and the metal complexes interact with DNA via non-intercalative binding. The competitive binding experiments with Hoechst 33258 indicated that 5-ASA and Cu complex could interact as groove binders, with fluorescence quenching on the fluorescence intensity and peak position of Hoechst-DNA system. Furthermore, Ni complex had no effect on the fluorescence intensity and peak position of MB-DNA system. The results obtained from experimental and molecular modeling showed good agreement.

#### Acknowledgements

Financial support from the Razi University Research Center is gratefully acknowledged.

#### Disclosure statement

No potential conflict of interest was reported by the authors.

## References

- [1] N. Raman, A. Selvan. *J. Mol. Struct.*, **985**, 173 (2011).
- [2] P.T. Selvi, H. Stoeckli-Evans, M. Palaniandavar. *J. Inorg. Biochem.*, **99**, 2110 (2005).
- [3] R.S. Kumar, S. Arunachalam. *Eur. J. Med. Chem.*, **44**, 1878 (2009).
- [4] R. Rao, A.K. Patra, P.R. Chetana. *Polyhedron*, **27**, 1343 (2008).
- [5] A.S. Abu-Surrah, M. Kettunen. *Curr. Med. Chem.*, **13**, 1337 (2006).
- [6] P. Bombicz, E. Forizs, J. Madarász, A. Deák, A. Kálmán. *Inorg. Chim. Acta*, **315**, 229 (2001).
- [7] G. Morgant, N. Bouhmaida, L. Balde, N.E. Ghermani, J. d'Angelo. *Polyhedron*, **25**, 2229 (2006).
- [8] R. Kurtaran, L.T. Yildirim, A.D. Azaz, H. Namli, O. Atakol. *J. Inorg. Biochem.*, **99**, 1937 (2005).
- [9] W. Luo, X. Meng, X. Sun, F. Xiao, J. Shen, Y. Zhou, G. Cheng, Z. Ji. *Inorg. Chem. Commun.*, **10**, 1351 (2007).
- [10] Z. Afrasiabi, E. Sinn, W. Lin, Y. Ma, C. Campana, S. Padhye. *J. Inorg. Biochem.*, **99**, 1526 (2005).
- [11] A. Buschini, S. Pinelli, C. Pellacani, F. Giordani, M.B. Ferrari, F. Bisceglie, M. Giannetto, G. Pelosi, P. Tarasconi. *J. Inorg. Biochem.*, **103**, 666 (2009).
- [12] N. Chitrapriya, V. Mahalingam, M. Zeller, K. Natarajan. *Inorg. Chim. Acta*, **363**, 3685 (2010).
- [13] N. Shahabadi, S. Moradi Fili, F. Kheiridoosh. *J. Photochem. Photobiol., B*, **128**, 20 (2013).
- [14] J. Sambrook, E.F. Fritsche, T. Maniatis. *Molecular Cloning: A Laboratory Manual*, 3rd Edn, Cold Spring Harbor Laboratory Press, Cold Spring Harbor, NY (1989).
- [15] G.D. Liu, J.P. Liao, Y.Z. Fang, S.S. Fang, G.L. Huang, R.Q. Sheng, J. Yu. *J. Anal. Sci.*, **18**, 391 (2002).
- [16] Sh Khan, F.B. Bux, A. Singh. *Der Pharmacia Lettre*, **4**, 57 (2010).
- [17] G.M. Morris, R. Huey, W. Lindstrom, M.F. Sanner, R.K. Belew, D.S. Goodsell, A.J. Olson. *J. Comput. Chem.*, **30**, 2785 (2009).
- [18] G.M. Morris, R. Huey, A.J. Olson, *Curr. Protoc. Bioinf.*, Chapter 8:Unit 8.14 (2008).
- [19] W. Humphrey, A. Dalke, K. Schulten. *J. Mol. Graphics*, **14**, 33 (1996).
- [20] *Spartan '10* (Package Windows Version), Wavefunction Inc., Irvine, CA (2011).
- [21] M. Shamsipur, M. Mohammadi, A. Taherpour, V. Lippolis, R. Montis. *Sens. Actuators, B*, **192**, 378 (2014).
- [22] A. Khatib, F. Aqra, D. Deamer, A. Oliver. *An. Asoc. Quim. Argent.*, **97**, 1 (2009).
- [23] N. Raman, S. Sobha. *Chem. Soc.*, **75**, 773 (2010).
- [24] Z.D. Qi, B. Zhou, Q. Xiao, C. Shi, Y. Liu, J. Dai. *J. Photochem. Photobiol., A: Chem.*, **193**, 81 (2008).
- [25] L.Z. Zhang, G.Q. Tang. *J. Photochem. Photobiol., B: Biol.*, **74**, 119 (2004).
- [26] A.M. Pyle, J.P. Rehmman, R. Meshoyrer, C.V. Kumar, N.J. Turro, J.K. Barton. *J. Am. Chem. Soc.*, **111**, 3053 (1989).
- [27] E.C. Long, J.K. Barton. *Acc. Chem. Res.*, **23**, 271 (1990).
- [28] S.R. Chowdhury, K.K. Mukherjea, R. Bhattacharyya. *Transition Met. Chem.*, **30**, 601 (2005).
- [29] F. Ahmadi, A.A. Alizadeh, F. Bakhshandeh-Saraskanrood, B. Jafari, M. Khodadadian. *Food Chem. Toxicol.*, **48**, 29 (2010).
- [30] N. Shahabadi, S. Hadidi. *Spectrochim. Acta, Part A*, **96**, 278 (2012).
- [31] V.I. Ivanov, L.E. Minchenkova, A.K. Schyolkina, A.I. Poletayev. *Biopolymers*, **12**, 89 (1973).
- [32] N. Poklar, D.S. Pilch, S.J. Lippard, E.A. Redding, S.U. Dunham, K.J. Breslauer. *Proc. Nat. Acad. Sci. USA*, **93**, 7607 (1996).
- [33] L.S. Lerman. *J. Mol. Biol.*, **3**, 18 (1961).
- [34] G. Zhang, P. Fu, J. Pan. *J. Lumin.*, **134**, 303 (2013).
- [35] M. Nandy, D.L. Hughes, G.M. Rosair, R.K.B. Singh, S. Mitra. *J. Coord. Chem.*, **67**, 3335 (2014).
- [36] Y. Zhang, G. Zhang, Y. Li, Y. Hu. *J. Agric. Food Chem.*, **61**, 2638 (2013).
- [37] Y. Sun, S. Bi, D. Song, C. Qiao, D. Mu, H. Zhang. *Sens. Actuators, B*, **129**, 799 (2008).
- [38] P.B. Kandagal, S. Shaikh, D. Manjunatha, J. Seetharamappa, B. Nagaralli. *J. Photochem. Photobiol., A*, **189**, 121 (2007).
- [39] Q. Wang, X. Wang, Z. Yu, X. Yuan, K. Jiao. *Int. J. Electrochem. Sci.*, **6**, 5470 (2011).
- [40] M. Jiang, M.X. Xie, D. Zheng, Y. Liu, X.Y. Li, X. Chen. *J. Mol. Struct.*, **692**, 71 (2004).
- [41] Y.J. Hu, H.G. Yu, J.X. Dong, X. Yang, Y. Liu. *Spectrochim. Acta, Part A*, **65**, 988 (2006).
- [42] N. Shahabadi, A. Fatahi. *J. Mol. Struct.*, **970**, 90 (2010).
- [43] N. Fani, A.K. Bordbar, Y. Ghayeb. *Spectrochim. Acta, Part A*, **103**, 11 (2013).
- [44] R. Kakkar, R. Garg. *J. Mol. Struct.*, **579**, 109 (2002).
- [45] J. Zhu, L. Chen, Y. Dong, J. Li, X. Liu. *Spectrochim. Acta, Part A*, **124**, 78 (2014).
- [46] Y. Guan, W. Zhou, X. Yao. *Anal. Chim. Acta*, **570**, 21 (2006).
- [47] S. Nafisi, A.A. Saboury, N. Keramat, J.F. Neault, H.A. Tajmir Riahi. *J. Mol. Struct.*, **827**, 35 (2006).
- [48] H. Li, X. Bu, J. Lu, C. Xu, X. Wang, X. Yang. *Spectrochim. Acta, Part A*, **107**, 227 (2013).
- [49] F. Perveen, R. Qureshi, A. Shah, S. Ahmed, F. Latif Ansari, S. Kalsoom, S. Mehboob. *Pharm. Chem. J.*, **1**, 1 (2011).
- [50] D. Khare, R. Pande. *Der Pharma Chemica*, **4**, 66 (2012).
- [51] M.L. Liu, M. Jiang, K. Zheng, Y.T. Li, Z.Y. Wu, C.W. Yan. *J. Coord. Chem.*, **67**, 630 (2014).